JOURNAL OF OPTOELECTRONICS AND ADVANCED MATERIALS Vol. 11, No. 12, December 2009, p. 1907 - 1914

Improving the structural description of high-temperature liquid $GeSe_2$ from ab initio molecular dynamics simulations

M. MICOULAUT*, C. MASSOBRIO[a]
Laboratoire de Physique Théorique de la Matière Condensée, Université Pierre et Marie Curie, Boite 121, 4, Place Jussieu, 75252 Paris Cedex 05, France
[a]*Institut de Physique et Chimie des Matériaux de Strasbourg, 23 rue du Loess, 67037 Strasbourg, France*

First-principles molecular dynamics simulations are performed on high temperature liquid $GeSe_2$ with two different gardient-corrected density functionals: the Perdue-Wang (PW) and the Becke, Lee, Yang and Parr (BLYP) functional. Structural and dynamical properties are analyzed and show a high influence depending on which is used. The BLYP functional not only increases the tetrahedral character of the system with a larger fraction of homopolor Ge-Ge bonding types, but also greatly affects the structure factor S(k) and the self-diffusion constants of the liquid. On the overall, this new functional brings the structural description closer to experimental findings determined from neutron diffraction.

(Received July 5, 2009; accepted November 12, 2009)

Keywords: Liquid $GeSe_2$, ab initio molecular dynamics

1. Introduction

Molecular Dynamics (MD) has appeared to be a method of choice for the description and the understanding at a microscpic level of the structural, dynamic and/or vibrational properties of stoichiometric network-forming liquids and glasses such as SiO_2, $SiSe_2$ or GeO_2. A certain number of studies have focused either on e.g. purely structural aspects [1-3], or on the relaxation dynamics related to the slowing down of the liquid close to its glass transition [4-6].

Among this class of systems, the relative successes of a classical MD is sometimes due to the nature of the chemical bonding (ionic or covalent) as a large difference in electronegativity between the components allows for charge separation and makes possible a classical description using Coulombic charges. Oxide tetrahedral liquids such as SiO_2 or GeO_2 belong to this category and corrections have been brought in order to treat more complex systems incorporating additives [7-8]. On the other hand, the simulation of chalcogenides with more weaker differences in electronegativities leading to an increased electronic charge transfer and an increased spatial extent of the electronic density, has shown important limitations [9-10] with classical descriptions. This has been the case for $GeSe_2$, although continuous refinements have been brought in the force fields. Experiments from neutron diffraction [11] show indeed the presence of defects made of homopolar bondings Ge-Ge and Se-Se which are not reproduced from MD. While this feature is completely absent in oxide glasses [12], the presence of homopolar bonding is acknowledged in chalcogenide liquids and glasses, their fraction increasing when moving down the Periodic Table, i.e. $GeSe_2$ has more homopolar defects [11] than GeS_2 [13]. Classical Born-Mayer potentials can often only provide heteropolar systems, and hardly succeed to produce structures with defects. Vashishta and co-workers [9] carried out a certain number of Molecular Dynamics simulations using classical interatomic potentials. More recently, Mauro and Varshneya, have fitted a new potential for the description of $GeSe_2$ which is able to produce some Se-Se defects in the glassy state [14], but no Ge-Ge bonds could be generated.

A more accurate description of the structural and vibrational properties of liquid and glassy $GeSe_2$ is certainly very timely as new interest has been brought to this compound and related alloys from an experimental viewpoint [15]. In fact, the binary Ge_xSe_{1-x} has proven to be a benchmark system for the understanding of a new elastic phase [16-18], an intermediate phase, discovered in the context of floppy to rigid transitions. This phase is found close to the network mean coordination number r=2.4 (corresponding to $GeSe_4$) where a rigidity transition from global Maxwell constraint counting is found [19]. This new phase displays some quite remakable properties such as the absence of ageing, a stress-free character and the vanishing of kinetic controlled enthalpies at the glass transition [15]. It is furthermore found in a variety of glasses including binary oxide and multicomponent electrolytes [20-21]. At this stage and even in the archetypal Ge_xSe_{1-x} glass system, it is not clear what originates the intermediate phase although phenomenological models [22, 23] and non-self-consistent

DFT calculations [24] have been proposed to understand its salient features. Any new insight from accurate first principles calculations can therefore provide structural clues for a better understanding of this intermediate phase. But before, there is need to improve the description of the stoichiometric $GeSe_2$, even in the liquid phase. This is the purpose of the present paper.

There have been continuous efforts to improve the density functional theory (DFT)-based description of $GeSe_2$. Effects of the density approximations have been studied [25] and highlighted the crucial effect played by approximation schemes for the XC (exchange-correlation), ranging from local density approximations (LDA) to Perdew-Wang (PW) generalized gradient approximation (GGA). For instance, it was shown that GGA with respect to LDA, would account for a better ionicity manifesting itself through a larger depletion of the valence charge density at Ge sites and a larger accumulation around Se atoms [25]. A consequence of this result was the complete absence, when using LDA, of a first sharp diffraction peak (FSDP) in the total structure factor S(k), in disagreement with experiment. Using the PW scheme, the structure of the liquid and the glass was found to display a good agreement [26,27] with experimental data although some limitations could be drawn: weak tetrahedral ordering, underestimation of homopolar defects, increased metallic character. Concerning the latter, one has to remark that the PW functional is a parameter-free gradient corrected functional which has been derived [28] from a consistent truncation of the gradient expansion of E_C, the reference state being the exact local correlation functional of the homogeneous electron gas. It therefore increases the delocalized behaviour of the valence electrons, i.e. increasing metallicity.

Having in hand the relative good agreement between theory and experiment from this PW-GGA based DFT scheme [26], can the accuracy of the electronic-based description be pushed one step forward ? The present article attempts to address this basic issue by comparing for high temperature liquid $GeSe_2$ the effect of two exchange-correlation functionals, the Perdew-Wang (PW) and the Becke, Lee, Yang and Parr (BLYP) functional. The latter attempts to optimize [29, 30] with one free parameter the correlation energy estimated from a Colle-Salveti formula [31], without any reference to the electron gas model. One therefore expects an increase of the electronic localization. We refer the reader to our recent work on low temperature liquid $GeSe_2$ (lt-$GeSe_2$) for a more detailed rationale [32] on the reasons underlying the present choice of the BLYP functional.

Our results show that, unlike lt-$GeSe_2$, the structure factors (total and to a lesser extent, partial) and the local structure (pair distribution functions, coordination numbers, fraction of homopolar bondings) are strongly sensitive to the choice of the functional, and bring a BLYP-based theory closer to the experimental findings [33]. Our paper is organized as follows. In Section 2, we describe our simulation method. Section 3 is devoted to the analysis of the partial and total structure factors and the comparison between experiment and theory from PW and BLYP. Section 4 focuses on the structure determined from the pair correlation functions, and analysis is given in terms of average coordination numbers and bond angle distributions. Section 5 provides some insight into the dynamical properties (diffusion constants). We finally conclude and summarize the main results of the paper.

2. Simulation details

The calculations were performed at constant volume on a system consisting of 40 germanium and 80 selenium atoms. A periodically repeated cubic cell of size 15.5 A was used to recover the exerimental density measured [34] in the liquid at 1373 K. The electronic structure has been described using DFT which evolves self-consistently during the motion. As already mentioned, two distinct exchange-correlation (PW and BLYP) functionals have been used. Valence electrons has been treated explicitely to account for core-calence interactions. For both functionals, the wave functions have been expanded at the Γ point of the super-cell on a plane-wave basis set defined by an energy cutoff E_c=20 Ry. The present choice of the cutoff appears to reproduce the main features of the low-vector limit of experimental partial structure factors and especially the FSDP. Details on the effect of the cutoff in $GeSe_2$ can be found in Refs. [26] and [27]. PW and BLYP functionals showed moderate differences on the Ge-Se dimer in bond lengths (respectively d_0=4.08 bohrs and 3.99 bohrs) and vibrational frequencies (ω=392 cm^{-1} and 398 cm^{-1}).

Additional computational details using the PW functional can be found in Ref. [26] and [27]. Concerning the BLYP functional, we used a fictious electron mass of μ_0=600 a.u. (in units of $m_e a_0^2$, where m_e is the electronic mass and a_0 is the Bohr radius) and a time step of δt=0.1 fs to integrate the equations of motion. Temperature control is implemented for both ionic and electronic degrees of freedom by using Nosé-Hoover thermostats [35, 36]. The simulations at T=1373 K were respectively carried out over time periods of 8 ps and 19 ps for the PW and BLYP functionals.

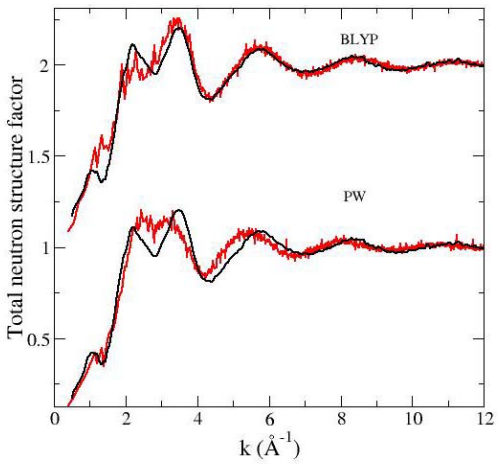

Fig. 1. Total neutron structure factors S(k) for liquid $GeSe_2$ using BLYP and PW calculations (red curves, [26] and present results), compared to experiments (black curves, from Refs. [33]).

3. Structure factors

The total structure factors for the two functionals are displayed in Fig. 1 and compared to experiments from neutron diffraction [33]. An correct agreement is found between the simulated BLYP total structure factor S(k) and the experimental one obtained by Penfold and Salmon. But while the improvement with respect to the PW scheme is obvious, we also notice that some salient features of the structure factor are still not well reproduced from a BLYP model. The latter leads indeed only to a shoulder contribution to the main peak for the first sharp diffraction peak (FSDP) found at k=1 $Å^{-1}$. On the other hand, the two main peaks observed at 2.2 $Å^{-1}$ and 3.5 $Å^{-1}$ are now clearly split from the simulation, in contrast with the PW-based description which showed [26] a single broad peak over the k-range of interest. We anticipate that the better agreement found at higher wave vector k for the BLYP functional should lead to a more accurate description of the local structure. Note finally that the system size (L= 15.5 Å) is sufficiently large to cover the low wave-vector region where the FSDP is observed as $k_{min}=2\pi/L=0.4$ $Å^{-1}$.

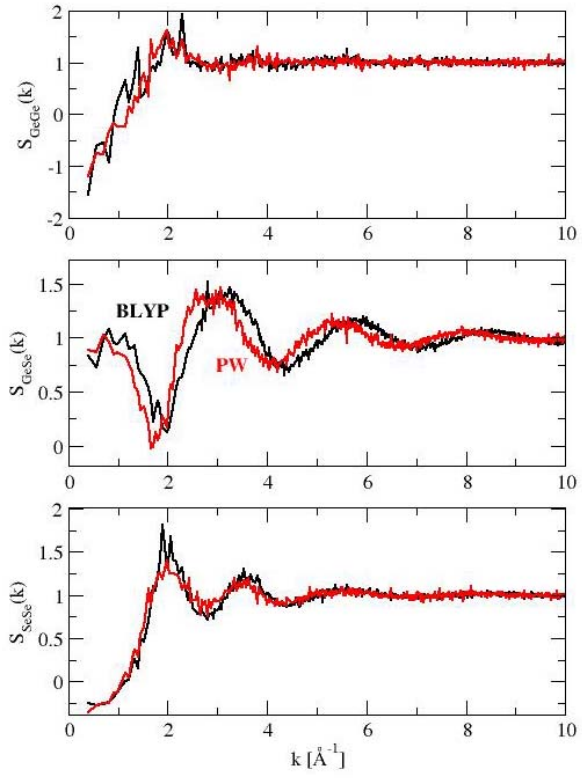

Fig. 2. Calculated Faber-Ziman partial structure factors : BLYP calculations (black) and PW calculations (red).

Additional insight is provided by the computation of partial structure factors $S_{ij}(k)$. In Fig. 2, we show the Faber-Ziman partials $S_{GeGe}(k)$, $S_{GeSe}(k)$ and $S_{SeSe}(k)$. Although the BLYP and PW-based partials are found to be very close, one can notice that the main difference arises from the Ge-Se correlations. In fact, from the panel representing $S_{GeSe}(k)$, it is seen the BLYP and PW curves are similar but shifted by about 0.2 $Å^{-1}$ to the smaller q values for PW, together with a broader peak found at around 3 $Å^{-1}$. These two features, shift and broadening, are responsible for the merging of the peaks observed experimentally in the total structure factor (fig. 1).

4. Real space properties: pair distribution functions and coordination numbers

The partial pair correlation functions $g_{ij}(r)$ are shown in Figure 3. A certain number of differences are found when considering the three functions. They also seriously contrast with the pair correlation functions found [32] at lower temperature (1050 K) for which the $g_{GeSe}(r)$ and $g_{SeSe}(r)$ using PW and BLYP have been found to be comparable. At the considered temperature of 1373 K, the global shape of all the partials is modified under the change of the exchange-correlation functional. One first notices that from the BLYP description, a well separated peak at 2.58 **Å** is obtained in the $g_{GeGe}(r)$ pair distribution function corresponding to the homopolar Ge-Ge bond, virtually absent in the PW calculations (fig. 3).

The presence of homopolar Ge defects in the stoichiometric compound $GeSe_2$ leads to a increase of local Ge-rich regions that need to be counterbalanced by homopolar Se-Se bonds. These are obtained for both descriptions (PW and BLYP) as manifested in the partial $g_{SeSe}(r)$ by a prepeak at 2.3 Å. The bond distances obtained from the other peak positions of the partials are found to differ slightly, i.e. we respectively find 3.94 Å (3.74 Å for PW), 2.38 Å (2.51 **Å** for PW) and 3.85 Å (3.85 Å for the PW, Ref [26]) for the Ge-Ge, Ge-Se and Se-Se bond distance. These findings are found to be in better agreement (respectively ~3.3, 2.40, and 3.80 Å) when compared to structural studies from neutron diffraction at the same temperature [33].

We finally remark that the minimum observed after the secondary peak at r ~ 3.6 Å in the Ge-Ge pair distribution function is much deeper for the BLYP model, similarly to what is observed for the Se-Se correlations where a pronounced minimum is found somewhat lower than 3.0 Å. On the overall, this means that the BLYP model leads to a slightly more structured liquid as the minimum between the first and second shell of neighbours is found to be deeper. It also brings the BLYP model closer to experimental findings [33] concerning the total pair distribution functions (Fig. 4). We obtain in fact a nearly complete agreement with a reproduction of almost all peak positions and heights, in contrast with the PW scheme. Short range (real space) and intermediate range (reciprocal space) are clearly improved with the BLYP functional.

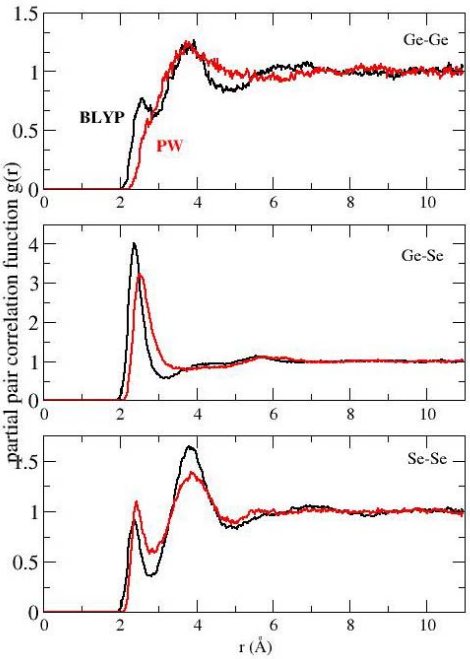

Fig. 3. Partial pair correlation function for liquid $GeSe_2$ at 1373 K: BLYP calculations (black), PW calculations (ref [26]).

We characterize a mean neighbourhood for the atomic species from the integration of the pair distribution functions which gives access to the respective coordination numbers n_{GeGe}, n_{GeSe} and n_{SeSe} where one has furthermore $n_{SeGe}=n_{GeSe}/2$. This allows the computation of the mean coordination number of the liquid defined by:

$$\overline{n} = c_{Ge}(n_{GeGe} + n_{GeSe}) + c_{Se}(n_{SeSe} + n_{SeGe}) \quad (1)$$

where c_{Ge} and c_{Se} represent respectively the concentration of germanium (33%) and selenium atoms (67/%). Having performed this computation over the same range of integration of the peaks as in [26] and [33], namely (2.09-3.01 **Å**), one obtains a mean coordination number from the BLYP estimation that is closer ($\overline{n} = 2.83$) to the experimental value [33] ($\overline{n} = 2.61$) than the computation obtained from PW ($\overline{n} = 2.95$).

Table 1. Coordination numbers extracted from the area of the first peaks in the pair distribution functions, compared to previous results using the PW functional [26] and the same integration range (2.09-3.01 Å).

	n_{SeSe}	n_{GeSe}	n_{GeGe}
BLYP (present study)	0.86	3.15	0.47
PW (Ref. [26])	1.08	3.19	0.32

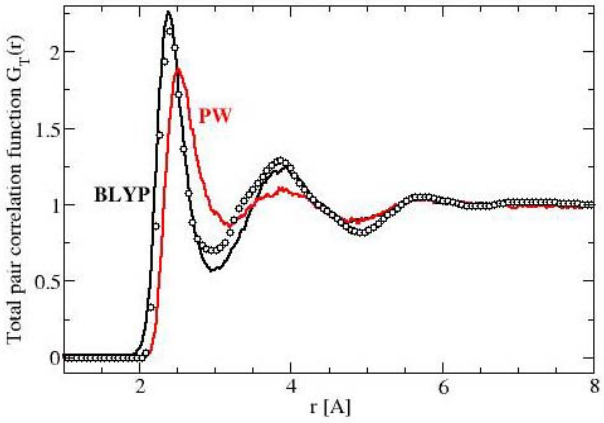

Fig. 4. Total pair distribution function from BLYP (black line) and PW (red line, Ref. [26]) calculations, compared to experimental results (circles, Ref [33]).

To gain an additional insight into the short range order of the liquid, and in order to fully characterize the local atomic environment, we define the quantity $n_\alpha(l)$ as the average number of atoms of species α that is l-fold coordinated, where α are Ge or Se atoms. A cut-off distance of 3 Å has been used to compute the coordination number from the first shell of neighbors. The present distance corresponds to the first minimum of the total pair distribution function (Fig. 4) and of the Ge-Se pair distribution function, but it is also close to the location of the obtained minima for the Ge-Ge and Se-Se correlations.

The comparison of the details of the local structure between BLYP and PW shows that the percentage of four-fold Ge atoms is substantially increased (49% against 37% with PW, fig. 5) but remains smaller than at lower temperature (1050 K, [26]). Our simulations contain a large amount of homopolar defects as manifested by an increased height and area of the first peak in the Ge-Ge pair distribution function. The increase of the fraction of four-fold germanium induces a decrease of the defect coordination *l=3* which is typical of the rocksalt GeSe phase [27] and whose signature is found experimentally in $GeSe_2$ from Mössbauer and Raman measurements [38]. The growth of this defect coordination in Ge_xSe_{1-x} with Ge composition *x* contributes together with the growth of homopolar bonding to a nanoscale phase separation and a reduction of the network connectivity which manifests in a maximum in the glass transition temperature [39] at *x=0.33*.

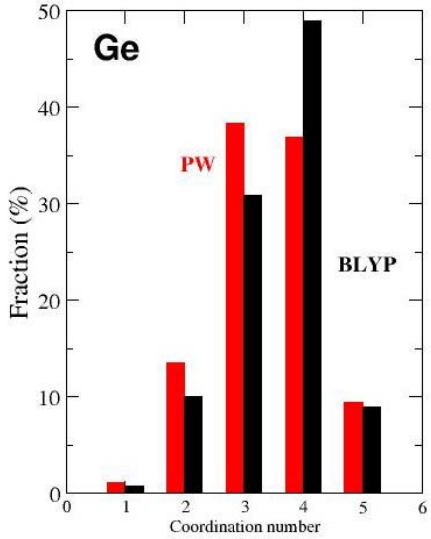

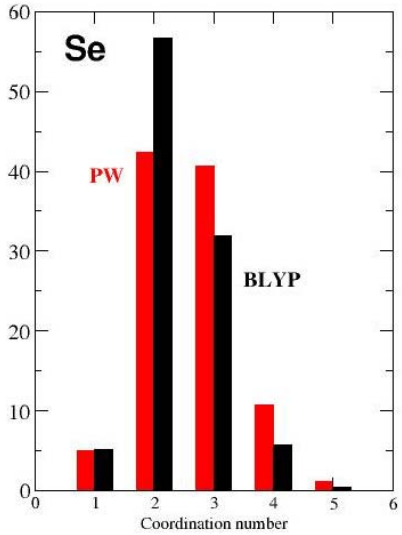

Fig. 5. Average number $n_{Ge}(l)$ and $n_{Se}(l)$ of Ge and Se atoms that are l-fold coordinated at a distance of 3 A in the liquid at 1373 K using the BLYP functional (PW results in red from Ref. [26]).

The selenium atoms show an increased preference for two-fold bonding (59% against 42 % for PW). This preference mostly leads to a growth of two-folded selenium atoms connecting to two germanium atoms (a Se-Ge_2 unit). Apart the one-fold defects, using BLYP all other possible coordinations ($n_{Se}(l)$ with l=3,4,5) are decreased with respect to the PW functional.

We finally show that temperature greatly affects the coordination number as shown in Figure 6. Here, one can see that over the 300 K interval between 1373 and 1050 K, the fraction of four-fold germanium and two-fold selenium atoms build up as usually expected in network glass-forming liquids [40]. We refer the reader to our work on lt-$GeSe_2$ for additional details on the local coordination numbers [32].

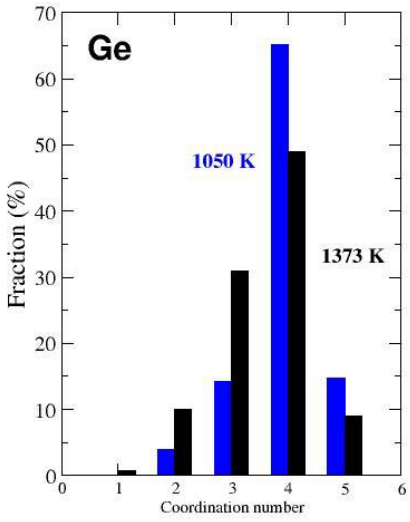

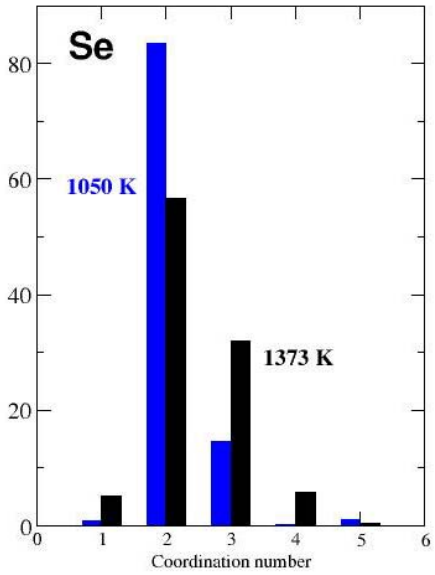

Fig. 6. Comparison of the obtained BLYP Ge and Se coordination numbers between 1050 K (blue, ref. [32]) and 1373 K (black, same as figure 5).

The computation of the bond angles shows that the bond angle distribution (BAD) is also very sensitive to the exchange-correlation functional. In fact, it is seen from Figure 7 that the bond angle Se-Ge-Se displays a proeminent peak at around 109^o of a symetric distribution for BLYP, against 103^o for PW. The presence of the angle at 109^o underscores the higher tetrahedral character of the BLYP-based liquid, a result that is in harmony with the results displayed in figure 5 showing the increased four-

fold coordination. Differences in the BAD emerges also from the Ge-Se-Ge component which provides a insight into the topology of the liquid, namely the different ways two tetrahedra can connect together. With a larger amount of angles in the range 100°-130°, one expects to have a more open structure with BLYP. The angles in liquid $GeSe_2$ have not been characterized but in the amorphous phase, it is usually found for Se-Ge-Se two contributions at 80° and 98° arising from edge- and corner-sharing tetrahedral [41]. Here it is found only a broad peak centred at around 100°, close to the low-temperature identified corner-sharing tetrahedral angle.

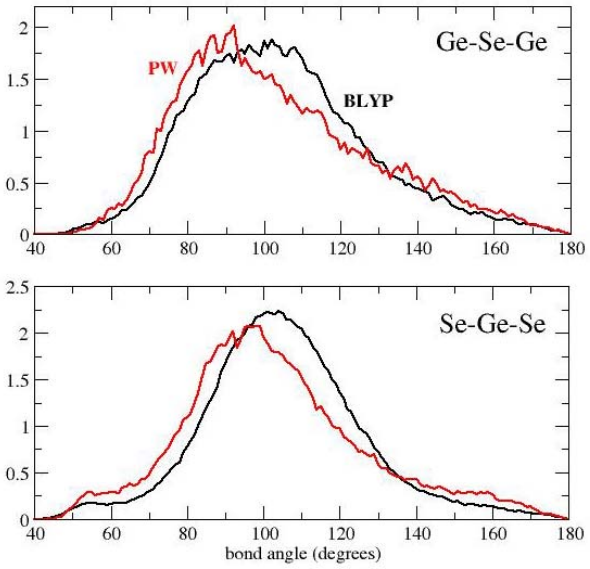

Fig. 7. Bond angle distribution of the 1373 K liquid $GeSe_2$ computed from PW (red curves, [26]) and BLYP functionals (black curves).

5. Dynamic properties

We finally focus on the transport properties by computing the mean-square displacement of a tagged atom of type a in the liquid:

$$\left\langle r^2(t)\right\rangle = \frac{1}{N_\alpha}\sum_{i=1}^{N_\alpha}\left\langle \left|r_i(t)-r_i(0)\right|\right\rangle \qquad (1)$$

with N_α is the number of atoms α.

The time dependence of this quantity for Ge and Se atoms is shown in Fig. 8 for the two temperatures 1050 K and 1373 K. In a log-log plot of the mean square displacement with time, the diffusive regime can be detected from a linear behaviour with a slope of one. Here, it is seen that for the high temperature liquid (1373 K), diffusion sets in after 2 ps, whereas it is only starting at the largest simulation time (40 ps) for the 1050 K BLYP liquid. The diffusion constant D can be obtained via the Einstein relation limit:

$$D = \frac{\left\langle r^2(t)\right\rangle}{6t} \qquad (2)$$

and corresponding Ge and Se diffusion constants extracted from Figure 8 are respectively $2.7\times10^{-5} cm^2\cdot s^{-1}$, and $2.2\times10^{-5} cm^2.s^{-1}$ for the 1373 K liquid, one order of magnitude larger than the diffusion constants found at 1050 K. One should note that for both temperatures, the diffusion constants of both Ge and Se atoms are about five times smaller with the BLYP scheme, when compared to PW.

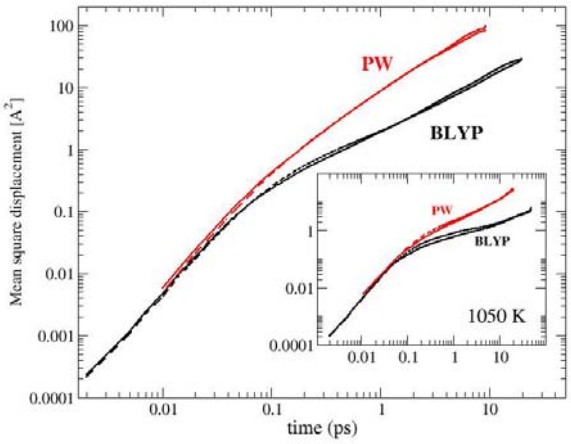

Fig. 8. Mean square displacement for Ge (solid) and Se (broken lines) at 1373 K with the BLYP (black) and PW (red, [26]) functionals. The insert shows the corresponding behaviour for the temperature T=1050 K ([27,32]).

How do these values compare with experimental data ? From this viewpoint, we are not aware of any published data but one can estimate rather accurately a mean diffusion constant from viscosity data [42] using the Eyring relation:

$$D = \frac{k_B T}{\eta\lambda} \qquad (3)$$

where λ is a typical hopping length for the diffusing atom [43]. In silicate melts e.g., Na_2SiO_3, Eq. (3) holds very well [44] with λ=2.8 Å, a distance typical of Si-Si and O-O separation in these melts. From viscosity data [45] of liquid $GeSe_2$, one is able to proceed in a similar way and deduce an average diffusion coefficient by postulating a reasonable value for the hopping length. Taking for λ a distance close to the Ge-Ge and Se-Se bond distance (3.7 Å), we obtain for the temperature 1373 K a diffusion coefficient equal to $2.54\times10^{-5} cm^2.s^{-1}$ which can be compared to the estimation of D_{Ge} and D_{Se} from the mean square displacement. It turns out that the BLYP model shows a better agreement with respect to this estimation.

The agreement is maintained in the lower temperature state.

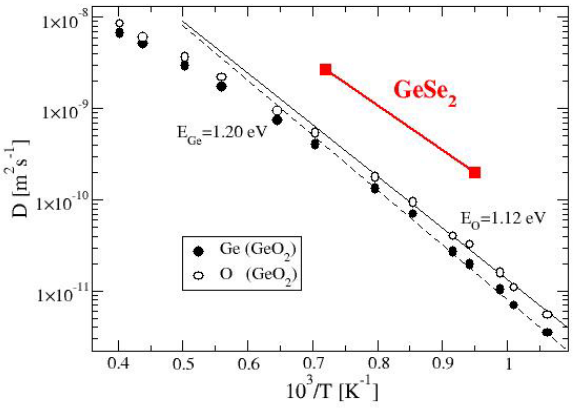

Fig. 9. Self-diffusion constant of simulated $GeSe_2$ (red) and GeO_2 (Ge: filled circles, O: open circles [46]) for as a function of inverse temperature. The two data points on the red line correspond to 1050 and 1373 K.

The present result can be compared to simulated diffusion constants [46] in liquid GeO_2. This comparison is made in Figure 9 where oxygen and germanium diffusion constants obtained from classical Molecular Dynamics are put in contrast with the present findings for $GeSe_2$ (D_{Ge}, red curves, similar to D_{Se}). It is found that at a given temperature, the diffusion constant of $GeSe_2$ is higher when compared to GeO_2, leading therefore (if one uses equ. (3)) to a lower viscosity.

We furthermore remark that, since both $GeSe_2$ and GeO_2 have the same slope in the figure, the related activation energy for Arrhenius-like diffusion for $GeSe_2$ is almost the same as the one found for GeO_2 (E_{Ge}=1.20 eV and E_O=1.12 eV). And as both glass-forming systems have a similar glass transition temperature (found to be respectively 850 K and 750 K for GeO_2 [47] and $GeSe_2$ [39]), one does expect that in an Angell plot representing the log of the viscosity with T_g/T, the viscosity curve of $GeSe_2$ will lie close but below the viscosity curve of GeO_2.

6. Summary and conclusions

A detailed structural analysis of high temperature liquid $GeSe_2$ using two exchange-correlation correlation functionals for the Kohn-Sham DFT calculation (PW and BLYP) has been reported. The first (PW) one is based on an extension of the uniform electronic gas approximation whereas the second one (BLYP) does not make any reference to this approximation and is expected therefore to enhance charge localisation properties. When comparing our results from BLYP to previous work devoted to this compound [26] using PW, we can clearly conclude that the former functional leads to an increased accuracy with respect to experimental data. Some clear features appear from this study. BLYP increases the tetrahedral character and the number of defects (homopolar Ge-Ge), consistently with recent findings at lower temperature [32]. It leads to an excellent agreement of the total pair distribution function when compared to experimental data. It also provides an estimate for the Ge and Se diffusion constants which are found to be close to and estimate from experimental data for viscosity.

In the high temperature liquid, BLYP appears to improve both the short-range (through the pair distribution function) and the long-range order (through the S(k). This situation contrasts with findings at lower temperature where the level of accuracy for the structure factor was found to be similar for both functionals.

Acknowledgements

The authors acknowledge ongoing discussions with P. Boolchand, A. Pasquarello, and P.S. Salmon.

References

[1] P. E. Poole, in Structure, Dyamics and Properties of Silicate Melts, edited by J. Stebbins, P. F. McMillan, and D. Dingwell, in Rev. Mineralogy Vol. 32, (Miner. Soc. America, Washington, D.C., 1995).
[2] B. Guillot and Y. Guissani, J. Chem. Phys. **104**, 7633 (1996).
[3] M. Micoulaut, J. Phys. Condens. Matt. **16**, L131 (2004).
[4] E. Zaccarelli, S. Andreev, F. Sciortino, D. R. Reichman, Phys. Rev. Lett. **100**, 195701 (2008).
[5] C. De Michele, P. Tartaglia, F. Sciortino, J. Chem. Phys. **125**, 204710, 2006
[6] A.J. Moreno, S. V. Buldyrev, E. La Nave, I. Saika-Voivod, F. Sciortino, P. Tartaglia, E. Zaccarelli, Phys. Rev. Lett. **95**, 157801 (2005)
[7] B. Guillot, N. Sator, Geochim. Cosmochim. Acta **71**, 1249 (2007).
[8] B.W.H. van Beest, G.J. Kramer, R.A. van Santen, Phys. Rev. Lett. **64**, 1955 (1990).
[9] P. Vashishta, G.A. Antonio, and I. Ebbsjô, Phys. Rev. Lett. **62**, 1651 (1989).
[10] P. Vashishta, R.K. Kalia, J.P. Rino, and I. Ebbsjô, Phys. Rev. **B{\bf 39},** 6034 (1989).
[11] I. Petri, and P.S. Salmon, Phys. Chem. Glasses **43C**, 185 (2002).
[12] P.S. Salmon, A.C. Barnes, R.A. Martin, G.J. Cuello, Phys. Rev. Lett. **96**, 235502 (2006).
[13] I. Petri, P.S. Salmon, J. Non-Cryst. Solids **293-295**, 169 (2001).
[14] J.C. Mauro and A.K. Varshneya, J; Am. Ceram. Soc. **89**, 2323 (2006).
[15] Rigidity and Boolchand phases in nanomaterials, M. Micoulaut and M. Popescu Eds. (INOE, 2009).
[16] P. Boolchand, X. Feng and W.J. Bresser, J.Non-Cryst. Solids., **293**, 348 (2001).

[17] X. Feng, W. Bresser, P. Boolchand, Phys. Rev. Lett. **78,** 4422 (1997).
[18] F. Wang, S. Mamedov, P. Boolchand, B. Goodman, M. Chandrasekhar, Phys. Rev**. B 71**, 174201 (2005).
[19] J.C. Phillips, J. Non-Cryst. Solids {\bf 43}, 37 (1981); M.F. Thorpe, J. Non-Cryst. Solids **57**, 355 (1983).
[20] Y. Vaills, T. Qu, M. Micoulaut, F. Chaimbault, P. Boolchand, J. Phys.: Condens. Matter **17**, 4889 (2005).
[21] D.I. Novita, P. Boolchand, M. Malki, and M. Micoulaut, Phys. Rev. Lett. **98**, 195501 (2007).
[22] M. Micoulaut, and J.C. Phillips, Phys. Rev. B **67**, 104204 (2003); M. Micoulaut, Phys. Rev. B **74**, 184208 (2006).
[23] M. V. Chubynsky, M. A. Briere, and N. Mousseau, Phys. Rev. E **74**, 016116 (2006).
[24] F. Inam, D. A. Drabold, M. Shatnawi, D. Tafen, P. Chen and S. Billinge, J. Phys. Cond. Matt. **19**, 455206 (2007).
[25] C. Massobrio, A. Pasquarello, and R. Carr, J. Am. Chem. Soc. **121**, 2943 (1999).
[26] C. Massobrio, F.H.M. Van Roon, A. Pasquarello, S.W. De Leeuw, J. Phys. Cond. Matt. **12**, L697 (2000).
[27] C. Massobrio, A. Pasquarello, and R. Carr, Phys. Rev. B **64**, 144205 (2001).
[28] J.P. Perdew, Y. Wang, Phys. Rev. B **45**, 13244 (1992).
[29] A.D. Becke, J. Chem. Phys. **96**, 9173 (1992).
[30] C. Lee, W. Yang, and R.C. Parr, Phys. Rev. B **37**, 785 (1988).
[31] R. Colle, D. Salvetti, Theor. Chim. Acta **37**, 329 (1975).
[32] M. Micoulaut, R. Vuilleumier and C. Massobrio, Phys. Rev. B **79**, 214205 (2009).
[33] I. Petri, P.S. Salmon, and S.W. Howells, J. Phys.: Cond. Matt. **11**, 10219 (1999).
[34] R. Ruska and H. Turn, J. Non-Cryst. Solids **22**, 277 (1976).
[35] S. Nosé, Mol. Phys. **52**, 255 (1984).
[36] W.G. Hoover, Phys. Rev. A **31**, 1695 (1985).
[37] I. Petri, P.S. Salmon, and H. Fischer, J. Non-Cryst. Sol. **250-252**, 405 (1999).
[38] P. Boolchand, and W.J. Bresser, Phil. Mag. **80**, 1757 (2000).
[39] P. Boolchand, D.G.Georgiev, T. Qu, F. Wang, L.Cai, S.Chakravarty. C. Rendus Chimie **5**, 713 (2002)
[40] P.S. Salmon, J. Non-Cryst. Solids **353**,2959 (2007).
[41] P. S. Salmon, J. Phys.: Condens. Matter **19**, 455208 (2007)
[42] A. Sipp and P. Richet, J. Non-Cryst. Solids **298**, 202 (2002)
[43] S. Glasstone, K. J. Laider, and H. Eyring, The Theory of Rate Processes, (McGraw-Hill, New York, 1941).
[44] B. O. Mysen and P. Richet, {\em Silicate Glasses and Melts: Structure and Properties} (Springer, Berlin, 2005).
[45] S. Stolen, T. Grande, and H-B. Johnsen, Phys. Chem. Chem. Phys. **4**, 3396 (2002).
[46] M. Micoulaut, Y. Guissani, B. Guillot, Physical Review E **73,** 031504 (2006)
[47] A. C. Wright, G. Etherington, J. A. Erwin Desa, R. N. Sinclair, G. A. N. Connel, and J. C. Mikkelson, J. Non-Cryst. Solids **49**, 63 (1982)

*Corresponding author: mmi@lptl.jussieu.ro;
Carlo.Massobrio@ipems.u-strasbg.fr